Bioorganic Chemistry 105 (2020) 104367

Contents lists available at ScienceDirect

Bioorganic Chemistry

journal homepage: www.elsevier.com/locate/bioorg

Discovery of natural alkaloids as potent and selective inhibitors against human carboxylesterase 2

Yi-Shu Zhao [1], Xing-Kai Qian [1], Xiao-Qing Guan, Pei-Fang Song, Yun-Qing Song, Rong-Jing He, Meng-Ru Sun, Xiu-Yang Wang, Li-Wei Zou [*], Guang-Bo Ge [*]

Institute of Interdisciplinary Integrative Medicine Research, Shanghai University of Traditional Chinese Medicine, Shanghai 201203, China

ARTICLE INFO

Keywords:
Alkaloids
Human carboxylesterase 2A (hCES2A)
Inhibitor
Reserpine

ABSTRACT

Human Carboxylesterase 2A (hCES2A), one of the most important serine hydrolases, plays crucial roles in the hydrolysis and the metabolic activation of a wide range of esters and amides. Increasing evidence has indicated that potent inhibition on intestinal hCES2A may reduce the excessive accumulation of SN-38 (the hydrolytic metabolite of irinotecan with potent cytotoxicity) in the intestinal tract and thereby alleviate the intestinal toxicity triggered by irinotecan. In this study, more than sixty natural alkaloids have been collected and their inhibitory effects against hCES2A are assayed using a fluorescence-based biochemical assay. Following preliminary screening, seventeen alkaloids are found with strong to moderate hCES2A inhibition activity. Primary structure–activity relationships (SAR) analysis of natural isoquinoline alkaloids reveal that the benzo-1,3-dioxole group and the aromatic pyridine structure are beneficial for hCES2A inhibition. Further investigations demonstrate that a steroidal alkaloid reserpine exhibits strong hCES2A inhibition activity (IC_{50} = 0.94 μM) and high selectivity over other human serine hydrolases including hCES1A, dipeptidyl peptidase IV (DPP-IV), butyrylcholinesterase (BChE) and thrombin. Inhibition kinetic analyses demonstrated that reserpine acts as a non-competitive inhibitor against hCES2A-mediated FD hydrolysis. Molecular docking simulations demonstrated that the potent inhibition of hCES2A by reserpine could partially be attributed to its strong σ-π and S-π interactions between reserpine and hCES2A. Collectively, our findings suggest that reserpine is a potent and highly selective inhibitor of hCES2A, which can be served as a promising lead compound for the development of more efficacious and selective alkaloids-type hCES2A inhibitors for biomedical applications.

1. Introduction

Mammalian carboxylesterases (CEs) are important members of the serine hydrolase superfamily (E.C. 3.1.1.1), which catalyze the hydrolysis of a variety of endogenous and exogenous compounds bearing ester bond(s) [1–3]. The carboxylesterase in humans can be divided into five subtypes, but the two main subtypes are human carboxylesterase 1A (hCES1A) and human carboxylesterase 2A (hCES2A). The amino acid sequences of hCES1A and hCES2A have 47% homology, and there are significant differences in substrate selectivity and tissue distribution [3–5]. hCES1A is mainly expressed in the liver and tends to hydrolyze substrates of small alcohol groups and large acyl groups such as enalapril, oseltamivir, imidazolidinium, clopidogrel [6–8]. However, hCES2A is mainly known as the enzyme expressed in the intestinal tract and involved in metabolism of large alcohol-based and small acyl substrates such as irinotecan, capecitabine, flutamide, procaine [9,10].

As the main carboxylesterase distributed in human intestine, hCES2A is considered to play an important role in the bioavailability of oral prodrugs and the therapeutic effect of some ester anticancer drugs [10,11]. For example, CPT-11, a carbamate prodrug prescribed for the

Abbreviations: ABS, absorbance; AMC, 7-amino-4-methylcoumarin; BAN, *N*-butyl-4-amino-1,8-naphthalimide; BChE, butyrylcholinesterase; BSA, bovine serum albumin; BTCH, butyrylthiocholine; BuchE, Butyrylcholinesterase; BuTChI, Butyrylcholine iodide; CEs, carboxylesterases; DME, D-luciferin methyl ester; DPP-IV, dipeptidyl peptidase IV; DTNB, 5,5′-dithiobis(2-nitrobenzoic acid); FD, fluorescent diacetate; hCES1A, human carboxylesterase 1A; hCES2A, human carboxylesterase 2A; HLM, human liver microsomes; LDR, Luciferin Detection Reagent; LPA, loperamide hydrochloride; 4-MUO, 4-Methylumbelliferyl oleate; SAR, structure–activity relationships; Z-GGRAMC, Z-Gly-Gly-Arg-AMC.

* Corresponding author.
E-mail addresses: chemzlw@163.com (L.-W. Zou), geguangbo@dicp.ac.cn (G.-B. Ge).
[1] These authors contribute equally to this work.

https://doi.org/10.1016/j.bioorg.2020.104367
Received 2 May 2020; Received in revised form 2 September 2020; Accepted 8 October 2020
Available online 12 October 2020
0045-2068/© 2020 Elsevier Inc. All rights reserved.

treatment of colorectal cancer, could trigger severe delayed diarrhea due to the overproduction of SN-38 (the hydrolytic product of CPT-11) in the small intestine. It is noteworthy that hCES2A can convert CPT-11 into SN-38 in the intestinal tract [12,13]. Therefore, it is hypothesized that co-administration with potent hCES2A inhibitors may ameliorate CPT-11 caused severe diarrhea in patients and thus reduce the suffering of patients [13,14]. In addition to the well-known roles of hCES2A in xenobiotic metabolism, the enzyme also participates in endogenous metabolism [15–17]. More recently, it has been reported that both triacylglycerol and diacylglycerol hydrolase activitys of hCES2A in liver are strongly related with several metabolic diseases, such as obesity and steatohepatitis [16]. Thus, hCES2A inhibitors can be used as co-drugs to modulate the hydrolysis of ester drugs and alter the pharmacokinetic profile of these drugs to increase the potency or reduce side effects of the hCES2A substrate drug [18,19], and also used as potential tools for exploring the biological functions of hCES2A in human being.

To date, biochemists have made significant breakthrough on the design and synthesis of several specific optical substrates for sensing the real activities of hCES1A or hCES2A in complex biological systems [20–27]. These newly developed optical substrates have been successfully used for high-throughput screening of natural inhibitors against CEs, such as flavonoids, tanshinones and triterpenoids [28–32]. Alkaloids, one of the largest classes of natural products, are nitrogen-containing compounds that occur naturally in various parts of plant including seeds, roots, flowers, leaves and fruits [33]. Currently, there are several marketed drugs available, which are alkaloidal in nature such as quinine [34], berberine [35] and morphine [36]. In addition, there are a large amount of alkaloids and their derivatives, which have been explored to achieve a potential lead for the drug development [37]. However, natural alkaloids inhibitors against hCES2A with high potency and enhanced selectivity are rarely reported [15]. In this present study, a series of alkaloids were collected and the inhibitory effects of these alkaloids on hCES2A were determined using fluorescent diacetate (FD) as substrate probe [20]. After preliminary screening, we found that seventeen alkaloids displayed good inhibitory effects against hCES2A. More in-depth researches on the inhibitory effects of these alkaloids against human carboxylesterases (CEs) were assayed using D-Luciferin methyl ester (DME) and FD as specific optical substrate for hCES1A, and hCES2A, respectively. It was found that the indole alkaloid reserpine has an excellent inhibitory effect on hCES2A and highly selectivity over hCES1A.

2. Experiments

2.1. Chemicals and reagents

All alkaloids were purchased from Chengdu Pufeide Biotechnology Co., Ltd. (Chengdu, China). Sodium chloride, galantamine hydrobromide and dabigatran etexilate were purchased from Dalian Meilun Biotechnology Co., Ltd. (Dalian, China). The purity of each standard compound was determined by LC-UV and its purity exceeded 98%. Human liver microsomes (HLM from 50 donors, lot X008067) were obtained from Bioreclamation IVT (Baltimore, MD, USA). Human plasma is perched from Research Institute for Liver Diseases (Shanghai) Ltd Co (RILD). Thrombin isolated from human plasma was purchased from HYPHEN BioMed (France, Lot F1700752P2). Fluorescent diacetate (FD, a fluorescent substrate for hCES2A) and loperamide hydrochloride (LPA) were purchased from TCI (Tokyo, Japan). The substrate of hCES1A, D-luciferin methyl ester (DME) and dipeptidyl peptidase IV (DPP-IV) substrate GP-BAN was synthesized in our laboratory [38,39]. Luciferin detection reagent (LDR) was purchased from Promega Biotech (Madison, USA). 4-Methylumbelliferyl oleate (4-MUO) was purchased from Sigma-Aldrich Co., Ltd (St. Louis, Missouri, USA). The fluorescent substrate for human thrombin, Z-Gly-Gly-Arg-AMC (Z-GGRAMC) acetate and bovine serum albumin (BSA) was purchased from Medchem Express (Shanghai, China). Butyrylcholine iodide (BuTChI) and 5,5′-dithiobis(2-nitrobenzoic acid) (DTNB) were purchased from Sigma-Aldrich. Substrate such as compound 1–68, FD, DME was dissolved in DMSO (Tedia, USA) and stored in a refrigerator at 4 ℃ until use. Phosphate buffered saline (0.1 M, pH 6.8 and pH 7.4), citrate-disodium hydrogen phosphate buffer (0.1 M, pH 7.4), Tris-HCl buffer (50 mM, pH 8.3) stored at 4 ℃, Millipore Water and LC grade acetonitrile (Tedia, USA) were used for all experiments.

2.2. Enzyme inhibition assays

2.2.1. hCES2A inhibition assay

The total volume of the system is 200 μL. The incubation system consisted of 2 μL of DMSO/inhibitor, 2 μL of human liver microsomes (2 μg/mL, final concentration), buffer PBS (pH = 7.4) 194 μL, substrate FD 2 μL (5 μM, final concentration). Set up three parallels. Three control groups were also established, the first being the non-inhibitor group (addition of an equal volume of DMSO with the inhibitor) as a 100% control of enzyme activity. The second was to determine background fluorescence for the HLM-free group (addition of an equal volume of PBS). The third group was a positive inhibitor group (loperamide, LPA). After incubating the system for 3 min, the substrate FD 2 μL was added, and after incubation for another 20 min, an equal volume of ice acetonitrile was added for inactivation. Pipette 200 μL into a black standard 96-well plate and place it in a fully automated fluorescent microplate reader (SpectraMax® iD3, Molecular Devices, Austria) for fluorescence analysis. The final concentration of DMSO is 1%. Residual activity (%) = (fluorescence intensity in the presence of inhibitor - blank fluorescence intensity per experimental group)/[fluorescence intensity of negative control (DMSO only) - blank fluorescence intensity of the experimental group in the presence of each inhibitor] × 100%.

2.2.2. hCES1A inhibition assay

The total volume of the system is 100 μL. The incubation system consisted of 2 μL of DMSO/inhibitor, 5 μL of human liver microsomes (1 μg / mL, final concentration), 91 μL of buffer PBS (pH = 6.5), 2 μL of substrate DME (3 μM, final concentration). Three concentrations (1 μM, 10 μM, 100 μM, final concentration) were established at the time of initial screening. Set up two groups of parallels. Three control groups were also established, the first being a non-inhibitor (addition of an equal volume of DMSO to the inhibitor) as a 100% control of enzyme activity. The second was to measure background fluorescence for the HLM microsomes (plus equal volumes of PBS).

After incubating the system for 3 min, DME was added, and after incubation for another 10 min, 50 μL of the solution was added, and 50 μL of LDR white standard 96-well plate was added and placed in a fully automated fluorescent microplate reader for chemiluminescence analysis. The final concentration of DMSO is 1%. Residual activity (%) = (fluorescence intensity in the presence of inhibitor - blank fluorescence intensity per experimental group)/[fluorescence intensity of negative control (DMSO only) - blank fluorescence intensity of the experimental group in the presence of each inhibitor] × 100%.

2.2.3. DPP-IV inhibition assay

The total volume of the system is 200 μL. The contents of the system were 2 μL of DMSO/inhibitor, 2 μL of human plasma, 194 μL of PBS (pH = 7.4), and 2 μL of substrate GP-BAN (100 μM, final concentration). Set up three parallels. Two control groups were also established, the first being the no-inhibitor group (addition of an equal volume of DMSO with the inhibitor) as a 100% control of enzyme activity. The second was to determine background fluorescence in the absence of DPP-IV (addition of an equal volume of PBS). After incubating the system for 3 min, the substrate GP-BAN 2 μL was added, and after incubation for another 20 min, an equal volume of ice acetonitrile was added for inactivation. Pipette 200 μL into a black standard 96-well plate and place it in a fully automated fluorescent microplate reader for fluorescence analysis. The excitation wavelength of the hydrolyzed metabolite (BAN) was set to

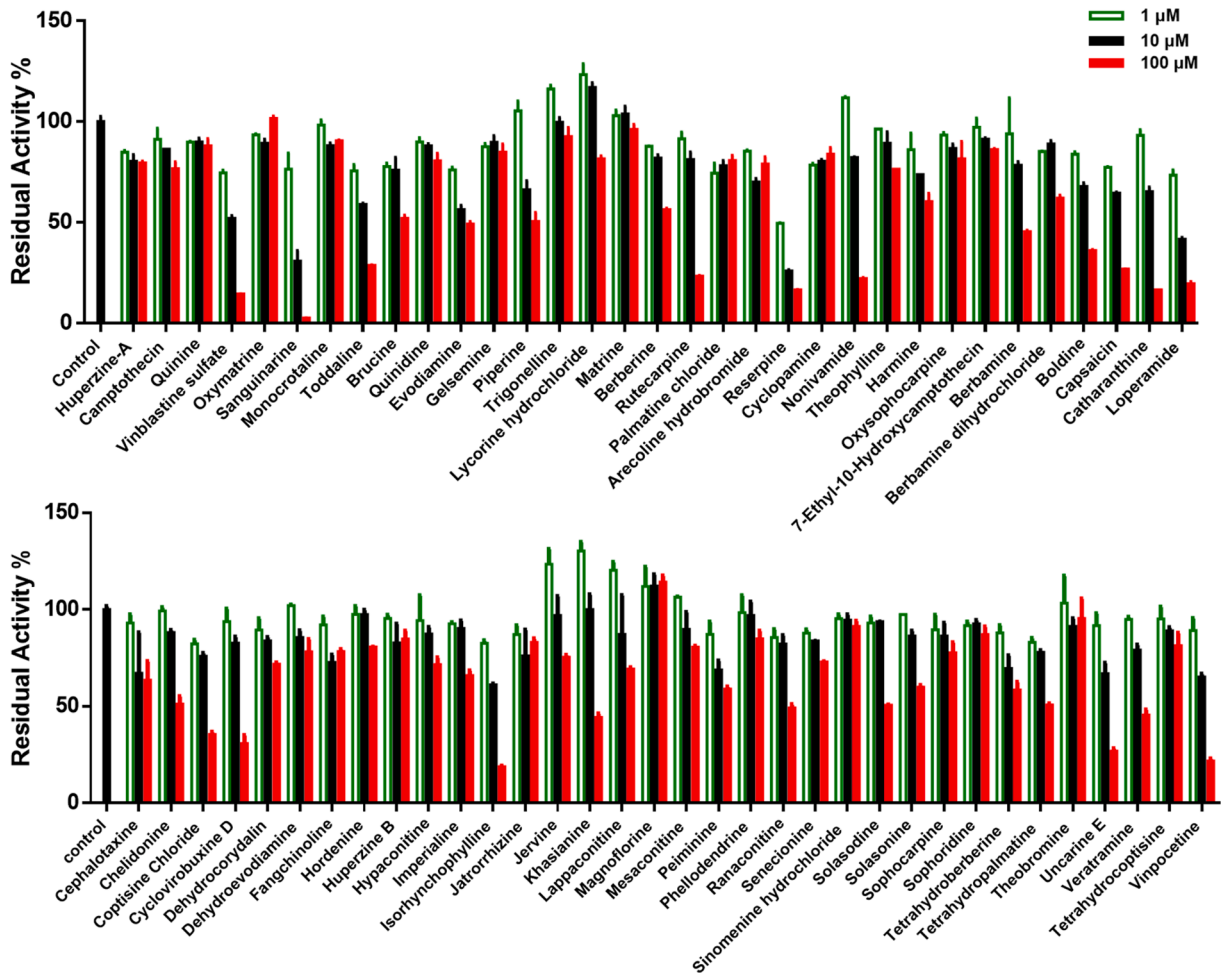

Fig. 1. Inhibition of hCES2A by alkaloids (final concentration 1 μM, 10 μM and 100 μM, respectively).

434 nm and the emission wavelength was 530 nm. The PMT gain value is set to 500. The final concentration of DMSO was 1%. Residual activity (%) = (fluorescence intensity in the presence of inhibitor - blank fluorescence intensity of the experimental group in the presence of each inhibitor)/[fluorescence intensity of negative control (DMSO only) - blank fluorescence intensity of the experimental group in the presence of each inhibitor] × 100%.

2.2.4. Thrombin inhibition assay

Experiments were performed in black standard 96-well plates. The total volume of the system is 200 μL. The contents of the system were 2 μL of DMSO/inhibitor, 2 μL of thrombin (0.1 NIH/mL, final concentration), 184 μL of buffer Tris-HCl (pH = 8.3, 50 mM), 2 μL of substrate Z-Gly-Gly-Arg-AMC (50 μM, final concentration), 10 μL of BSA (0.1 mg/mL, final concentration). Set up three parallels. Three control groups were also established, the first being the non-inhibitor group (addition of an equal volume of DMSO with the inhibitor) as a 100% control of enzyme activity. The second was the background of the thrombin-free group (addition of an equal volume of Tris-HCl) to determine background fluorescence. The third group was the positive inhibitor group (dabigatran etexilate, 10 μM, final concentration). After incubating the system for 3 min, 2 μL of the substrate Z-Gly-Gly-Arg-AMC was added and placed in a fully automated fluorescent microplate reader for fluorescence analysis. The fluorescence detection conditions were Ex 380 nm/Em 440 nm. The fluorescent signal of the hydrolyzed metabolite (7-amino-4-methylcoumarin, AMC) was recorded by a microplate reader at intervals of 60 s. Take the fluorescence value of 20 min. The final concentration of DMSO was 1%. The residual activity of human thrombin was calculated by the following formula, residual activity (%) = (fluorescence intensity of AMC in the presence of inhibitor - blank fluorescence intensity of the experimental group in the presence of each inhibitor)/[negative control (DMSO only) fluorescence intensity of medium AMC - blank fluorescence intensity of the experimental group in the presence of each inhibitor] × 100%.

2.2.5. Butyrylcholinesterase (BuchE) inhibition assay

Experiments were performed in clear 96-well plates. The total volume of the system is 100 μL. System contents were 2 μL of DMSO/inhibitor, 2 μL of human serum, 84 μL of buffered PBS (pH = 7.4, 0.1 M), 10 μL of substrate iodized butyrylthiocholine (300 μM, final concentration), 2 μL of developer 5–5′-dithiobis(2-nitrobenzoic acid) (DTNB) (1000 μM, final concentration). Set up three parallels. Three control groups were also established, the first being the non-inhibitor group (addition of an equal volume of DMSO with the inhibitor) as a 100% control of enzyme activity. The second was the butyrylcholinesterase group (addition of an equal volume of PBS) to determine background fluorescence. The third group was the positive inhibitor group (galantamine hydrobromide, 10 μM, final concentration). The BTCH of this experiment was dissolved in Millipore water (3 mM, initial concentration). After incubating the system for 3 min, 10 μL of the substrate BTCH was added, and the product absorbance (ABS) value was measured by a fully automatic fluorescent microplate reader. The ABS of the product was measured at a wavelength of 412 nm, a time interval of 60 s, and a detection time of 20 min. The final concentration of DMSO was 1%. After the test is completed, the slope of the test result is calculated. The residual activity of butyrylcholinesterase was calculated by the

Table 1
The IC_{50} values of alkaloids toward hCES1A and hCES2A.

	IC_{50} (hCES2A) (μM)	IC_{50} (hCES1A) (μM)	Selectivity
1	5.76 ± 0.76	>100	>17.36
2	30.06 ± 11.83	>100	>3.33
3	13.40 ± 5.41	>100	>7.46
4	39.18 ± 14.64	>100	>2.55
5	>100	>100	–
6	>100	>100	–
7	>100	>100	–
8	>100	>100	–
9	>100	>100	–
10	>100	>100	–
11	>100	>100	–
12	>100	>100	–
13	5.90 ± 0.82	>100	>16.94
14	0.94 ± 0.12	>100	>106.38
15	12.85 ± 0.90	8.88 ± 0.63	0.69
16	16.90 ± 3.02	>100	>5.91
17	5.94 ± 0.89	35.34 ± 3.08	5.94
18	7.03 ± 0.75	87.59 ± 17.24	12.46
19	30.97 ± 7.78	49.93 ± 14.55	1.61
20	6.53 ± 1.04	>100	>15.31
21	13.33 ± 2.44	>100	>7.50
22	24.20 ± 4.41	>100	>4.13
23	25.82 ± 7.13	>100	>3.87
24	27.83 ± 4.91	>100	>3.59
25	35.05 ± 3.79	>100	>2.85
LPA[b]	1.72 ± 0.28	>100	>58.13

Selectivity is calculated from IC_{50} (hCES1A)/IC_{50} (hCES2A).
[a]All experimental data are averages of at least three independent experiments.
[b] LPA: Loperamide, a positive inhibitor against carboxylesterases.

following formula, residual activity (%) = (slope in the presence of inhibitor)/[slope of negative control (DMSO only)] × 100%.

2.3. Inhibition kinetic analyses

A set of inhibition kinetics of reserpine against hCES2A-mediated FD hydrolysis has been carefully investigated. The inhibition constant (K_i) value was determined using various concentrations of FD in the presence of different concentrations of reserpine. To determine the type of inhibition kinetics (competitive inhibition, non-competitive inhibition, and mixed inhibition), various concentrations of inhibitor and different substrates were used to determine the corresponding reaction rates. The function of the inhibitor is from the second plot of the slope of the Lineweaver-Burk plot for calculating the corresponding inhibition constant (K_i) value.

2.4. Molecular docking simulations

The structure of hCES2A was downloaded from the SWISS-MODEL library (a database of annotated 3D protein structure models generated by homology modeling pipeline) [40]. Molecular docking was performed using AutoDock Vina version 1.1.2 [41]. The crystallized waters were removed, and the protein was assigned polar hydrogens and united atom Kollman charges. The docking grid was generated with a volume of 80 × 80 × 80 and centered at the catalytic triad (Ser228, Glu345, and His457). The docking simulation was carried out based on the Lamarckian genetic algorithm. The protein–ligand pose with the lowest binding energy was displayed in full text.

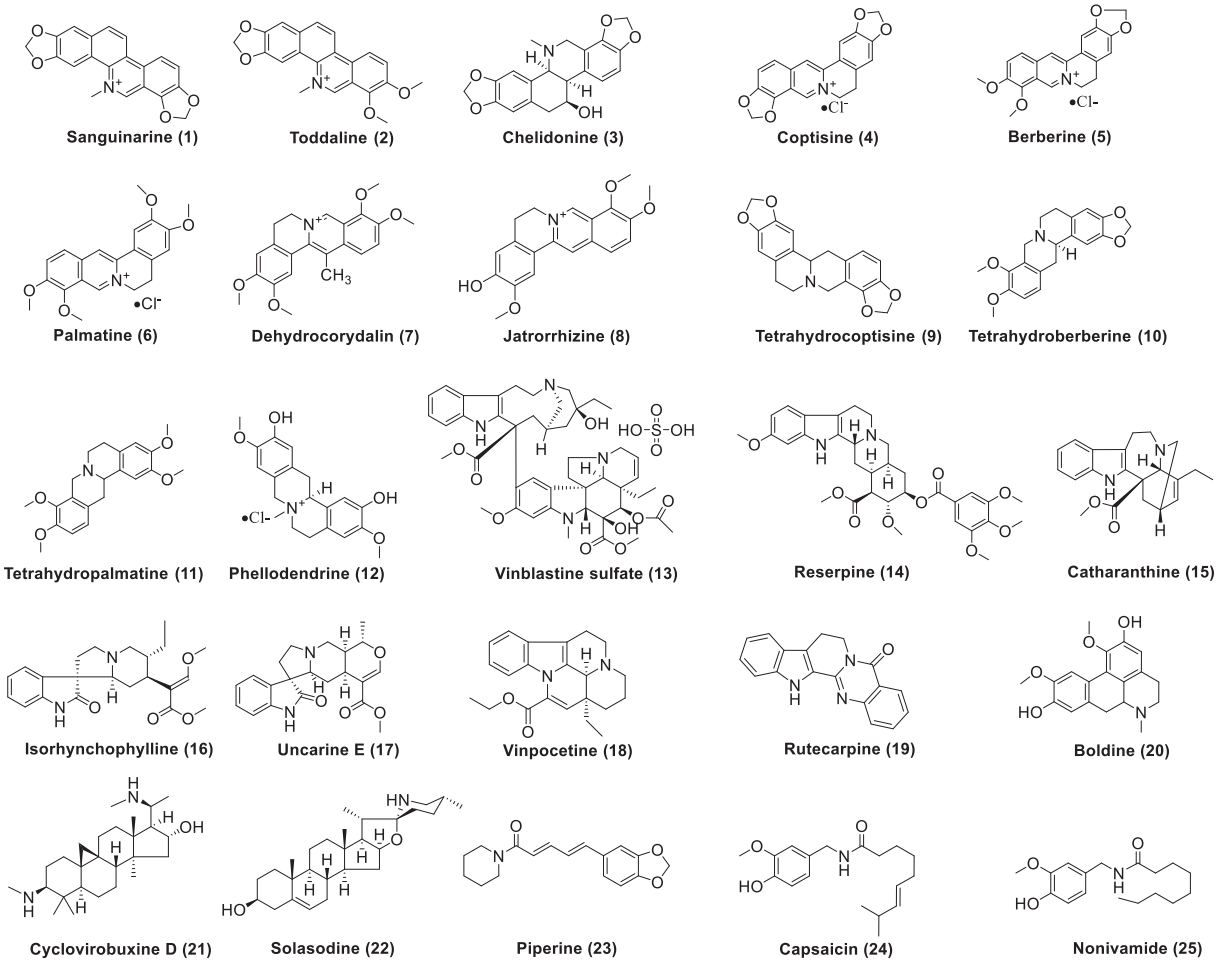

Fig. 2. Chemical structures of alkaloids with hCES2A inhibition activity.

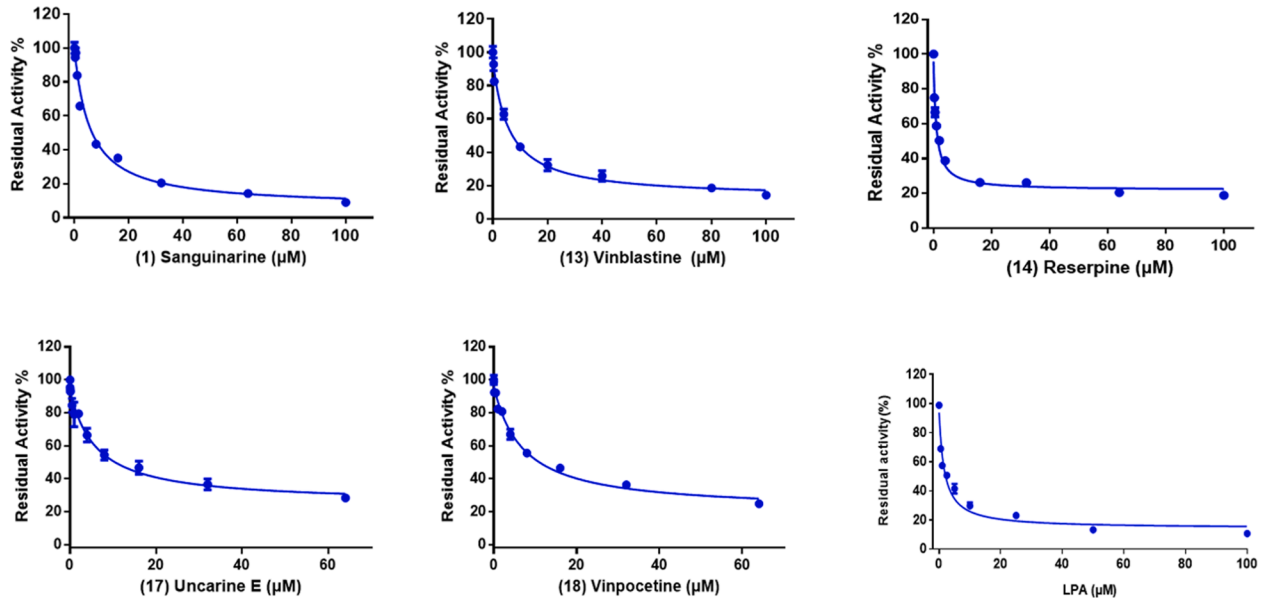

Fig. 3. The dose-inhibition curves of five alkaloids with potent hCES2A inhibition activity.

2.5. Statistical analysis

All measurements were performed in triplicate, and the results presented here are all based on the mean ± SD. IC_{50} values were determined by non-linear regression using GraphPad Prism 6.0 software.

3. Results and discussion

3.1. Inhibitory potentials of natural alkaloids against hCES2A

Our previous studies have developed several specific activity-based optical probe substrates for hCES1A and hCES2A, which have been successfully used for rapid screening and characterization of inhibitors against CEs [42–44]. In this study, sixty-six natural alkaloids were collected and FD was used as a substrate probe for preliminary screening of these alkaloids inhibitory effect on hCES2A using three inhibitor concentrations (1 μM, 10 μM and 100 μM). It is evident from Fig. 1 that most of tested natural alkaloids displayed weak inhibitory effects or without any inhibitory effects on hCES2A even at the high concentration (100 μM). There were seventeen alkaloids displaying good inhibitory effects against hCES2A. Further studies on the inhibitory effects of these alkaloids against hCES2A were assayed using FD as specific optical substrate. The bioassay results are summarized in Table 1. Sanguinarine (**1**), vinblastine sulfate (**13**), uncarine E (**17**), vinpocetine (**18**) and boldine (**20**) displayed strong inhibitory effects on hCES2A with lower IC_{50} value about 5 μM. Reserpine (**14**) showed excellent inhibitory effect against hCES2A with much lower IC_{50} value of 0.94 μM. In addition, a known inhibitor loperamide (LPA) was tested under identical conditions as positive control for hCES2A. The result indicated that LPA showed inferior inhibitory effect on hCES2A in contrast to reserpine (**14**). The dose-dependent inhibition curves of reserpine (**14**), sanguinarine (**1**), vinblastine sulfate (**13**), uncarine E (**17**) and vinpocetine (**18**) against hCES2A mediated FD hydrolysis are shown in Fig. 3.

Table 2
IC_{50} values of reserpine toward hCES1A, hCES2A, DPP-IV, BChE and thrombin.

IC_{50} (μM)				
hCES2A	hCES1A	BChE	DPP-IV	Thrombin
0.94 ± 0.12	>100	>100	>100	>100

3.2. SAR analysis of isoquinoline alkaloids

Isoquinoline alkaloids, a diverse group of natural products, have been exploited for medicinal and toxic properties, leading up to a source of numerous drugs and drug precursors used as pharmaceutics [45–49]. Twelve isoquinoline alkaloids (compound **1**–**12**) were assayed for their inhibitory effects against hCES2A (Fig. 2). It is evident from Table 1 that sanguinarine (**1**) displayed good inhibitory effect on hCES2A (IC_{50}, 5.76 μM). Toddaline (**2**) exhibited relatively lower inhibitory effect on hCES2A (IC_{50}, 30.06 μM) compared with sanguinarine (**1**), suggesting that the benzo-1,3-dioxole group in sanguinarine (**1**) structure is good for hCES2A inhibition. Chelidonine (**3**) and coptisine (**4**) displayed moderate inhibitory effects on hCES2A with IC_{50} vales of 13.40 μM and 39.18 μM, respectively. As compared with coptisine (**4**), compound **5**–**8** exhibit poor inhibitory effects on hCES2A, indicating that the phthalic ether substitute is unbeneficial for hCES2A inhibition. Tetrahydrocoptisine (**9**) with hydropyridine unit could not inhibit hCES2A (IC_{50} > 100 μM), indicating that the hydropyridine group introduced in such isoquinoline alkaloid is not beneficial for inhibitory property toward hCES2A. Consistently, compound **10**–**12** exhibited similar trends in hCES2A inhibition as tetrahydrocoptisine (**9**). Based on the primary structure–activity relationships (SAR) analysis of isoquinoline alkaloids **1**–**12,** we could conclude that the benzo-1,3-dioxole group and the aromatic pyridine structure are very essential for hCES2A inhibition. For other alkaloids compounds **13**–**66**, we did not obtain a clear SAR due to the large difference of the structural classes and the disorganized structural connectivity of these compounds.

3.3. Selectivity of reserpine towards hCES2A over other human serine hydrolases

The inhibitory effects of alkaloids on hCES1A were routinely screened using three inhibitor concentrations (1 μM, 10 μM, 100 μM) and using D-Luciferin methyl ester (DME) as specific optical substrate. As shown in Supporting Information Fig. 1, a majority of tested alkaloids displayed weak inhibitory effects on hCES1A even at the high concentration (100 μM), only a few compounds showed relative moderate inhibition potentials on hCES1A-mediated DME hydrolysis. The further bioassay results are summarized in Table 1. Reserpine (**14**) was found with strong inhibitory effect on hCES2A (IC_{50}, 0.94 μM) and high selectivity over hCES1A (>100-fold). In order to further prove that

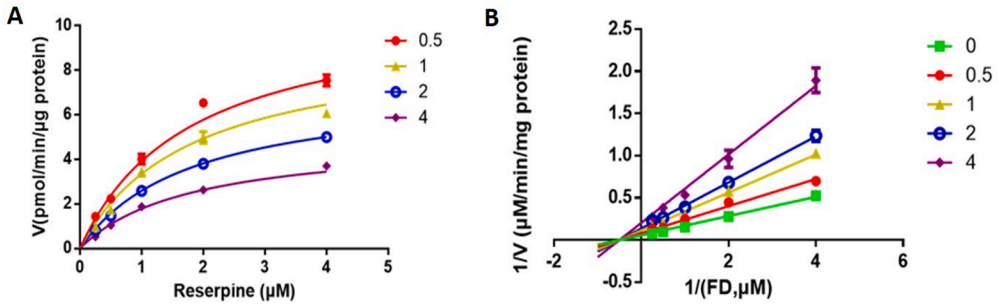

Fig. 4. (A) Enzymatic kinetics of FD and Michaelis-Menten equation; (B) The Lineweave-Burk plot of reserpine against hCES2A-mediated FD.

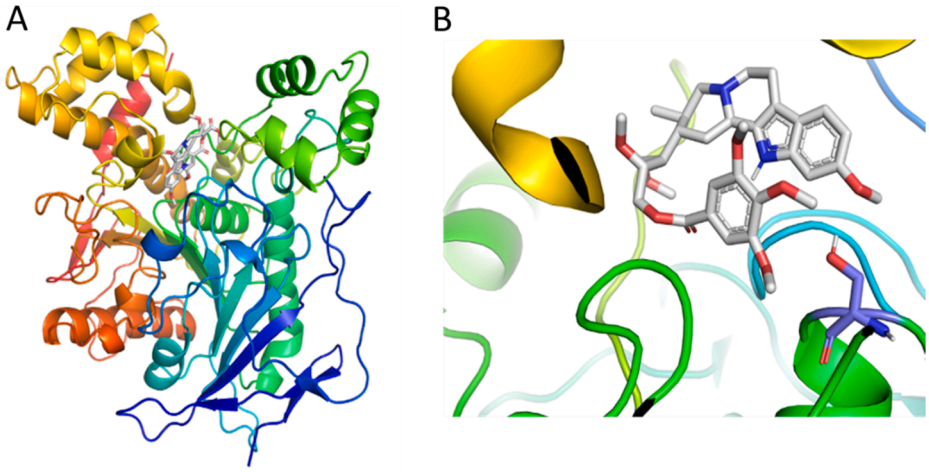

Fig. 5. (A) A stereogram of the structure hCES2A and of reserpine; (B) A detailed view of the orientation of reserpine (**14**) in hCES2A active sites.

reserpine (**14**) is a higher selective inhibitor on hCES2A than other serine hydrolases, the inhibitory effects of reserpine (**14**) against other human serine hydrolase including dipeptidyl peptidase IV (DPP-IV), butyrylcholinesterase (BChE) and thrombin were carried out according to the known assays [31,50,51]. As shown in Table 2, reserpine **(14)** has a poor inhibitory effect on these serine hydrolases, with IC_{50} values >100. This indicates that reserpine (**14**) is a specific inhibitor of hCES2A.

3.4. Inhibition kinetic analyses

The strong inhibition potency of reserpine (**14**) against hCES2A encouraged us to further investigate the inhibition mechanism of this natural alkaloid toward hCES2A. As shown in Fig. 4, Lineweaver-Burk plots demonstrated that reserpine could inhibit hCES2A in HLMs *via* a non-competitive inhibition, with K_i value of 1.53 μM.

3.5. Molecular docking simulations

To explore the interaction mode between reserpine (**14**) and hCES2A, molecular docking was carried out. The ligand pose with the lowest binding energy in complex of hCES2A was analyzed. As shown in the Fig. 5A, reserpine (**14**) could favorably interact with the active site gorge of hCES2A, and the main interactions are hydrophobic forces shown in Supporting Information Fig. 2. Residue Ala150 located at the bottom of the gorge could form a σ-π interaction with 3,4,5-trimethoxy aromatic group. Also, Met354 near the entrance of the gorge could form a S-π interaction with the same aromatic group on the other side. The NH group of Phe307 could form a hydrogen bond with the oxygen atom of the methyl ester moiety. These findings agreed well with the experimental data where reserpine (**14**) exhibited much more potent inhibitory effect on hCES2A.

4. Conclusions

In summary, sixty-six natural alkaloids were collected and their inhibitory effects against both hCES1A and hCES2A were assayed. Seventeen alkaloids displayed strong to moderate inhibition against hCES2A. The structure–activity relationships (SAR) analysis of isoquinoline alkaloids **1**–**12** is well summarized and discussed. The SAR results show that the benzo-1,3-dioxole group and the aromatic pyridine structure are very essential for hCES2A inhibition. The alkaloid reserpine (**14**) was found to have a strong inhibitory effect on hCES2A mediated FD hydrolysis, with an IC_{50} value of about 0.94 μM and selectivity to other human serine hydrolase including hCES2A, DPP-IV, BChE and thrombin. In addition, the inhibition kinetic analyses demonstrated that reserpine (**14**) was a non-competitive inhibitor against hCES2A-mediated FD hydrolysis. Molecular docking indicated that the σ-π and S-π interaction formed by 3,4,5-trimethoxy aromatic group of reserpine (**14**) and Ala150 and Met354 of hCES2A, the hydrogen bond formed by methyl ester moiety of reserpine (**14**) and Phe307 of hCES2A could consistent with the potent inhibitory effect of reserpine (**14**) against hCES2A.

Declaration of Competing Interest

The authors declare that they have no known competing financial interests or personal relationships that could have appeared to influence the work reported in this paper.

Acknowledgements

Authors are grateful to the National Science and Technology Major Project of China (2018ZX09731016), the NSF of China (81703604, 81803489 and 81773687) and the National Key Research and Development Program of China (2017YFC1702000, 2017YFC1700200).

Appendix A. Supplementary material

Supplementary data to this article can be found online at https://doi.org/10.1016/j.bioorg.2020.104367.

References

[1] M. Hosokawa, T. Maki, T. Satoh, Characterization of molecular species of liver microsomal carboxylesterases of several animal species and humans, Arch. Biochem. Biophys. 277 (1990) 219–227.
[2] P. Ellinghaus, U. Seedorf, G. Assmann, Cloning and sequencing of a novel murine liver carboxylesterase cDNA, Biochim. et Biophys. Acta - Gene Struct. Expression 1397 (1998) 175–179.
[3] T. Satoh, M. Hosokawa, Carboxylesterases: structure, function and polymorphism in mammals, J Pestic Sci 35 (2010) 218–228.
[4] J.A. Crow, A. Borazjani, P.M. Potter, M.K. Ross, Hydrolysis of pyrethroids by human and rat tissues: Examination of intestinal, liver and serum carboxylesterases, Toxicol. Appl. Pharm. 221 (2007) 1–12.
[5] M.K. Ross, J.A. Crow, Human Carboxylesterases and their role in xenobiotic and endobiotic metabolism, J. Biochem. Mol. Toxic. 21 (2007) 187–196.
[6] M. Hosokawa, Structure and catalytic properties of carboxylesterase isozymes involved in metabolic activation of prodrugs, Molecules 13 (2008) 412–431.
[7] T. Satoh, P. Taylor, W.F. Bosron, S.P. Sanghani, M. Hosokawa, B.N. La Du, Current progress on esterases: From molecular structure to function, Drug Metab. Dispos. 30 (2002) 488–493.
[8] H.J. Zhu, X.W. Wang, B.E. Gawronski, B.J. Brinda, D.J. Angiolillo, J.S. Markowitz, Carboxylesterase 1 as a Determinant of Clopidogrel Metabolism and Activation, J. Pharmacol. Exp. Ther. 344 (2013) 665–672.
[9] H. Yano, S. Kayukawa, S. Iida, C. Nakagawa, T. Oguri, T. Sanda, J. Ding, F. Mori, A. Ito, M. Ri, A. Inagaki, S. Kusumoto, T. Ishida, H. Komatsu, H. Inagaki, A. Suzuki, R. Ueda, Overexpression of carboxylesterase-2 results in enhanced efficacy of topoisomerase I inhibitor, irinotecan (CPT-11), for multiple myeloma, Cancer Sci. 99 (2008) 2309–2314.
[10] N. Ribelles, J. Lopez-Siles, A. Sanchez, E. Gonzalez, M.J. Sanchez, F. Carabantes, P. Sanchez-Rovira, A. Marquez, R. Duenas, I. Sevilla, E. Alba, A carboxylesterase 2 gene polymorphism as predictor of capecitabine on response and time to progression, Curr. Drug Metab. 9 (2008) 336–343.
[11] G. Xu, W.H. Zhang, M.K. Ma, H.L. McLeod, Human carboxylesterase 2 is commonly expressed in tumor tissue and is correlated with activation of irinotecan, Clin. Cancer Res. 8 (2002) 2605–2611.
[12] M.K. Ma, H.L. McLeod, Lessons learned from the irinotecan metabolic pathway, Curr. Med. Chem. 10 (2003) 41–49.
[13] R.M. Wadkins, J.L. Hyatt, K.J.P. Yoon, C.L. Morton, R.E. Lee, K. Damodaran, P. Beroza, M.K. Danks, P.M. Potter, Discovery of novel selective inhibitors of human intestinal carboxylesterase for the amelioration of irinotecan-induced diarrhea: Synthesis, quantitative structure-activity relationship analysis, and biological activity, Mol. Pharmacol. 65 (2004) 1336–1343.
[14] L.D. Hicks, J.L. Hyatt, S. Stoddard, L. Tsurkan, C.C. Edwards, R.M. Wadkins, P. M. Potter, Improved, Selective, Human Intestinal Carboxylesterase Inhibitors Designed to Modulate 7-Ethyl-10- 4-(1-piperidino)-1-piperidino carbonyloxycamptothecin (Irinotecan; CPT-11) Toxicity, J. Med. Chem. 52 (2009) 3742–3752.
[15] D.D. Wang, L.W. Zou, Q. Jin, J. Hou, G.B. Ge, L. Yang, Human carboxylesterases: a comprehensive review, Acta Pharm. Sin. B 8 (2018) 699–712.
[16] M.A. Ruby, J. Massart, D.M. Hunerdosse, M. Schonke, J.C. Correia, S.M. Louie, J. L. Ruas, E. Naslund, D.K. Nomura, J.R. Zierath, Human Carboxylesterase 2 Reverses Obesity-Induced Diacylglycerol Accumulation and Glucose Intolerance, Cell Rep. 18 (2017) 636–646.
[17] Y.Y. Li, M. Zalzala, K. Jadhav, Y. Xu, T. Kasumov, L.Y. Yin, Y.Q. Zhang, Carboxylesterase 2 Prevents Liver Steatosis by Modulating Lipolysis, Endoplasmic Reticulum Stress, and Lipogenesis and Is Regulated by Hepatocyte Nuclear Factor 4 Alpha in Mice, Hepatology 63 (2016) 1860–1874.
[18] K.J.P. Yoon, J.L. Hyatt, C.L. Morton, R.E. Lee, P.M. Potter, M.K. Danks, Characterization of inhibitors of specific carboxylesterases: Development of carboxylesterase inhibitors for translational application, Mol. Cancer Ther. 3 (2004) 903–909.
[19] M.J. Hatfield, P.M. Potter, Carboxylesterase inhibitors, Expert Opin. Ther. Pat. 21 (2011) 1159–1171.
[20] J. Wang, E.T. Williams, J. Bourgea, Y.N. Wong, C.J. Patten, Characterization of Recombinant Human Carboxylesterases: Fluorescein Diacetate as a Probe Substrate for Human Carboxylesterase 2, Drug Metab. Dispos. 39 (2011) 1329–1333.
[21] M. Shimizu, T. Fukami, M. Nakajima, T. Yokoi, Screening of Specific Inhibitors for Human Carboxylesterases or Arylacetamide Deacetylase, Drug Metab. Dispos. 42 (2014) 1103–1109.
[22] Z.M. Liu, L. Feng, J. Hou, X. Lv, J. Ning, G.B. Ge, K.W. Wang, J.N. Cui, L. Yang, A ratiometric fluorescent sensor for highly selective detection of human carboxylesterase 2 and its application in living cells, Sensor Actuat. B-Chem. 205 (2014) 151–157.
[23] Q. Jin, L. Feng, D.D. Wang, Z.R. Dai, P. Wang, L.W. Zou, Z.H. Liu, J.Y. Wang, Y. Yu, G.B. Ge, J.N. Cui, L. Yang, A Two-Photon Ratiometric Fluorescent Probe for Imaging Carboxylesterase 2 in Living Cells and Tissues, ACS Appl. Mater. Interf. 7 (2015) 28474–28481.
[24] Q. Jin, L. Feng, D.D. Wang, J.J. Wu, J. Hou, Z.R. Dai, S.G. Sun, J.Y. Wang, G.B. Ge, J.N. Cui, L. Yang, A highly selective near-infrared fluorescent probe for carboxylesterase 2 and its bioimaging applications in living cells and animals, Biosens. Bioelectron. 83 (2016) 193–199.
[25] D.D. Wang, Q. Jin, J. Hou, L. Feng, N. Li, S.Y. Li, Q. Zhou, L.W. Zou, G.B. Ge, J. G. Wang, L. Yang, Highly sensitive and selective detection of human carboxylesterase 1 activity by liquid chromatography with fluorescence detection, J. Chromatogr. B Anal. Technol. Biomed. Life Sci. 1008 (2016) 212–218.
[26] L.L. Ding, Z.H. Tian, J. Hou, Z.M. Weng, J.N. Cui, L. Yang, G.B. Ge, Design and development of fluorescent probe substrates for carboxylesterase 1 using BODIPY as the basic fluorophore, Acta Pharm. Sin. B 52 (2017) 58–65.
[27] Y.S. Zhao, H.L. Ruan, X.Y. Wang, C. Chen, P.F. Song, C.W. Lü, L.W. Zou, Catalyst-free visible-light-induced condensation to synthesize bis(indolyl)methanes and biological activity evaluation of them as potent human carboxylesterase 2 inhibitors, RSC Adv. 9 (2019) 40168–40175.
[28] P.F. Song, Y.D. Zhu, H.Y. Ma, Y.N. Wang, D.D. Wang, L.W. Zou, G.B. Ge, L. Yang, Discovery of natural pentacyclic triterpenoids as potent and selective inhibitors against human carboxylesterase 1, Fitoterapia 137 (2019), 104199.
[29] D.D. Wang, L.W. Zou, Q. Jin, J. Hou, G.B. Ge, L. Yang, Recent progress in the discovery of natural inhibitors against human carboxylesterases, Fitoterapia 117 (2017) 84–95.
[30] L.W. Zou, Y.G. Li, P. Wang, K. Zhou, J. Hou, Q. Jin, D.C. Hao, G.B. Ge, L. Yang, Design, synthesis, and structure-activity relationship study of glycyrrhetinic acid derivatives as potent and selective inhibitors against human carboxylesterase 2, Eur. J. Med. Chem. 112 (2016) 280–288.
[31] L.W. Zou, Q. Jin, D.D. Wang, Q.K. Qian, D.C. Hao, G.B. Ge, L. Yang, Carboxylesterase Inhibitors: An Update, Curr. Med. Chem. 25 (2018) 1627–1649.
[32] L.W. Zou, T.Y. Dou, P. Wang, W. Lei, Z.M. Weng, J. Hou, D.D. Wang, Y.M. Fan, W. D. Zhang, G.B. Ge, L. Yang, Structure-Activity Relationships of Pentacyclic Triterpenoids as Potent and Selective Inhibitors against Human Carboxylesterase 1, Front. Pharmacol. 8 (2017) 435.
[33] K. Patel, V. Kumar, D.K. Patel, An update of therapeutic potential and bioanalytical aspects of steroidal glycoalkaloid (solanidine), J. Coastal Life Med. 5 (3) (2017) 134–140.
[34] H.M. Faidallah, S.S. Panda, J.C. Serrano, A.S. Girgis, K.A. Khan, K.A. Alamry, T. Therathanakorn, M.J. Meyers, F.M. Sverdrup, C.S. Eickhoff, S.G. Getchell, A. R. Katritzky, Synthesis, antimalarial properties and 2D-QSAR studies of novel triazole-quinine conjugates, Bioorg. Med. Chem. 24 (2016) 3527–3539.
[35] Y. Zhang, X. Wang, L. Liu, N. Chai, Q. Li, K. Wu, The anti-diarrhea mechanisms of berberine in diarrhea disease, Shaanxi Yixue Zazhi 39 (2010) 6–8.
[36] R.S. Sinatra, J.S. Jahr, J.M. Watkins-Pitchford, The essence of analgesia and analgesics, Cambridge University Press, 2010, pp. 82–90.
[37] J.C. Lewis, R.G. Bergman, J.A. Ellman, Direct functionalization of nitrogen heterocycles via Rh-catalyzed C-H bond activation, Acc. Chem. Res. 41 (2008) 1013–1025.
[38] L.W. Zou, P. Wang, X.K. Qian, L. Feng, Y. Yu, D.D. Wang, Q. Jin, J. Hou, Z.H. Liu, G.B. Ge, L. Yang, A highly specific ratiometric two-photon fluorescent probe to detect dipeptidyl peptidase IV in plasma and living systems, Biosens. Bioelectron. 90 (2017) 283–289.
[39] D.D. Wang, Q. Jin, L.W. Zou, J. Hou, X. Lv, W. Lei, H.L. Cheng, G.B. Ge, L. Yang, A bioluminescent sensor for highly selective and sensitive detection of human carboxylesterase 1 in complex biological samples, Chem. Commun. 52 (2016) 3183–3186.
[40] A. Waterhouse, M. Bertoni, S. Bienert, G. Studer, G. Tauriello, R. Gumienny, F. T. Heer, T.A.P. de Beer, C. Rempfer, L. Bordoli, R. Lepore, T. Schwede, SWISS-MODEL: homology modelling of protein structures and complexes, Nucleic Acids Res. 46 (2018) W296–W303.
[41] Z. Wang, H.Y. Sun, X.J. Yao, D. Li, L. Xu, Y.Y. Li, S. Tian, T.J. Hou, Comprehensive evaluation of ten docking programs on a diverse set of protein-ligand complexes: the prediction accuracy of sampling power and scoring power, PCCP 18 (2016) 12964–12975.
[42] X.Z. Bao, S.Q. Wei, L.W. Zou, Y.M. Song, J.P. Qu, B.M. Wang, Asymmetric fluorination of 4-substituted pyrazolones catalyzed by quinine, Tetrahedron Asymmetry 27 (2016) 436–441.
[43] X.Z. Bao, S.Q. Wei, X.K. Qian, J.P. Qu, B.M. Wang, L.W. Zou, G.B. Ge, Asymmetric Construction of a Multi-Pharmacophore-Containing Dispirotriheterocyclic Scaffold and Identification of a Human Carboxylesterase 1 Inhibitor, Org. Lett. 20 (2018) 3394–3398.
[44] F.Z. Han, B.B. Su, P.F. Song, Y.Q. Wang, L.N. Jia, S.S. Xun, M.G. Hu, L.W. Zou, N-bromosuccinimide mediated decarboxylative sulfonylation of beta-keto acids with sodium sulfinates toward beta-keto sulfones: Evaluation of human carboxylesterase 1 activity, Tetrahedron 74 (2018) 5908–5913.
[45] S.K. Mantena, S.D. Sharma, S.K. Katiyar, Berberine, a natural product, induces G (1)-phase cell cycle arrest and caspase-3-dependent apoptosis in human prostate carcinoma cells, Mol Cancer Ther 5 296-308.
[46] A. Shirwaikar, A. Shirwaikar, K. Rajendran, I.S.R. Punitha, In vitro antioxidant studies on the benzyl tetra isoquinoline alkaloid berberine, Biol. Pharm. Bull. 29 (2006) 1906–1910.

[47] L. Grycova, J. Dostal, R. Marek, Quaternary protoberberine alkaloids, Phytochemistry 68 (2007) 150–175.
[48] M. Asai, N. Iwata, A. Yoshikawa, Y. Aizaki, S. Ishiura, T.C. Saido, K.J.B. Maruyama, B.R. Communications, Berberine alters the processing of Alzheimer's amyloid precursor protein to decrease Aβ secretion, Biochem. Biophys. Res. Commun. 352 (2007) 498–502.
[49] M. Imanshahidi, H. Hosseinzadeh, Pharmacological and therapeutic effects of Berberis vulgaris and its active constituent, berberine, Phytother. Res. 22 (2008) 999–1012.
[50] Y.K. Yoon, M.A. Ali, A.C. Wei, T.S. Choon, K.Y. Khaw, V. Murugaiyah, H. Osman, V.H. Masand, Synthesis, characterization, and molecular docking analysis of novel benzimidazole derivatives as cholinesterase inhibitors, Bioorg. Chem. 49 (2013) 33–39.
[51] X. Yu, L.H. Wei, J.K. Zhang, T.R. Chen, Q. Jin, Y.N. Wang, S.J. Zhang, T.Y. Dau, Y. F. Cao, W.Z. Guo, G.B. Ge, L. Yang, Anthraquinones from Cassiae semen as thrombin inhibitors: in vitro and in silico studies, Phytochemistry 165 (2019), 112025.